Original article

High-speed large-scale automated isolation of SARS-CoV-2 from clinical samples using miniaturized co-culture coupled to high-content screening

Rania Francis [1, 2], Marion Le Bideau [2], Priscilla Jardot [2], Clio Grimaldier [2], Didier Raoult [1, 2], Jacques Yaacoub Bou Khalil [1, *], Bernard La Scola [1, 2, *]

[1] Institut Hospitalo-Universitaire Méditerranée-Infection, Marseille, France
[2] Aix-Marseille Université, Institut de Recherche pour le Développement (IRD), UMR Microbes Evolution Phylogeny and Infections (MEPHI), AP-HM, Marseille, France

ARTICLE INFO

ABSTRACT

Objectives: A novel coronavirus, severe acute respiratory syndrome coronavirus 2 (SARS-CoV-2), is responsible for the current coronavirus disease 2019 global pandemic. Only a few laboratories routinely isolate the virus, which is because the current co-culture strategy is highly time-consuming and requires a biosafety level 3 laboratory. This work aimed to develop a new high-throughput isolation strategy using novel technologies for rapid and automated isolation of SARS-CoV-2.
Methods: We used an automated microscope based on high-content screening (HCS), and we applied specific image analysis algorithms targeting cytopathic effects of SARS-CoV-2 on Vero E6 cells. A randomized panel of 104 samples, including 72 that tested positive by RT-PCR and 32 that tested negative, were processed with our HCS strategy and were compared with the classical isolation procedure.
Results: The isolation rate was 43% (31/72) with both strategies on RT-PCR-positive samples and was correlated with the initial RNA viral load in the samples, in which we obtained a positivity threshold of 27 Ct. Co-culture delays were shorter with the HCS strategy, where 80% (25/31) of the positive samples were recovered by the third day of co-culture, compared with only 26% (8/30) with the classic strategy. Moreover, only the HCS strategy allowed us to recover all the positive samples (31 with HCS versus 27 with classic strategy) after 1 week of co-culture.
Conclusions: This system allows the rapid and automated screening of clinical samples with minimal operator workload, which reduces the risk of contamination and paves the way for future applications in clinical microbiology, such as large-scale drug susceptibility testing. **Rania Francis, Clin Microbiol Infect 2021;27:128.e1—128.e7**
© 2020 European Society of Clinical Microbiology and Infectious Diseases. Published by Elsevier Ltd. All rights reserved.

Introduction

An outbreak caused by the novel coronavirus severe acute respiratory syndrome coronavirus 2 (SARS-CoV-2) occurred in late December 2019 in Wuhan, China; it then spread worldwide and was declared a pandemic by the WHO on 12 March 2020 [1—3].

Laboratory diagnosis is mainly based on molecular biology using specific RT-PCR systems to detect the virus in clinical samples [4—6]. However, during pandemics, strain isolation is important because having the particle represents the key to all *in vitro* research, such as drug susceptibility testing and vaccine development [7]. Furthermore, culture allows access to all viral genomes, as whole-genome sequencing techniques performed directly on samples have their limitations in terms of sensitivity.

A first application of this strategy was used by our group to evaluate the risk of contagiousness of patients before their discharge from the infectious diseases ward [8]. However, the current co-culture strategy is tedious and time consuming,

* Corresponding authors. Bernard La Scola, Jacques Yaacoub Bou Khalil, Aix Marseille Université, IRD, APHM, MEPHI, IHU-Méditerranée Infection, 19–21 boulevard Jean Moulin, 13005 Marseille, France.
E-mail addresses: boukhaliljacques@gmail.com (J.Y. Bou Khalil), bernard.la-scola@univ-amu.fr (B. La Scola).

especially because of the large number of samples to be cultured. An ideal solution would be an automated system allowing the rapid screening and monitoring of co-cultures on a large scale.

In previous works, we developed a screening strategy based on high-content screening microscopy (HCS) for the isolation of environmental giant viruses in amoebae and the strict intracellular bacterium *Coxiella burnetii* [9,10]. In this work, we used the same automated high-throughput method and adapted it for SARS-CoV-2 isolation from clinical samples with the objective to discard the negative co-cultures after 1 week and omit blind subcultures. Specific algorithms were applied to detect cytopathic effects in co-cultures at high throughput, which eliminates the subjectivity related to manual observations by laboratory personnel. This strategy exhibited a similar isolation rate but a lower co-culture delay when compared with the classic technique that is routinely used for isolation, as we were able to detect all positive co-cultures in 1 week.

Methods

Co-culture process for the developmental stage

For protocol development, we used Vero E6 cells (ATCC CRL-1586) as cellular support and the locally isolated SARS-CoV-2 strain IHUMI-3. This viral strain was previously isolated in our laboratory from a nasopharyngeal swab, as previously described [11]. The viral titre was calculated by the $TCID_{50}$ method. Briefly, we cultured Vero E6 cells in black 96-well microplates with optical bottoms (Nunc, Thermo Fisher, Waltham, MA, USA) at a concentration of 2×10^5 cells/mL and a volume of 200 µL per well in transparent minimum essential medium supplemented with 4% fetal calf serum and 1% glutamine. Plates were incubated for 24 hours at 37°C in a 5% CO_2 atmosphere to allow cell adhesion. Infection was then carried out with 50 µL of the viral stock suspension diluted up to 10^{-10}. The plates were centrifuged for 1 hour at 700 ***g***, and the total volume per well was adjusted to 250 µL with culture medium. Uninfected cells were considered negative controls.

Detection process optimization

DNA staining was performed with NucBlue™ Live ReadyProbes™ reagent (Molecular Probes, Life Technologies, Carlsbad, CA, USA). A concentration of 4 ng/mL was used (equivalent to 10 µL per well directly from stock solution), and a different well was stained each day to avoid photobleaching and possible cytotoxicity, as previously described [10].

Image acquisition and analysis were performed using the automated CellInsight™ CX7 High-Content Analysis Platform coupled with an automation system including an Orbitor™ RS Microplate mover and an incubator Cytomat™ 2C-LIN (Thermo Scientific). The HCS Studio 3.1 software was used to set up acquisition parameters using a 20 × objective (0.45 NA) and to define image analysis. Autofocus was performed on the fluorescence channel of the fluorescent probe NucBlue (386 nm). This channel served as a primary mask for cell detection and identification. The regions of interest were then identified on bright-field images as a Voronoi diagram derived from nuclear masks. Cell debris was removed using area cut-offs. The entire well (80 fields per well) was screened on a daily basis, and data were extracted and analysed in a dedicated application that we recently developed in R Studio® for the detection of the intracellular bacteria *Coxiella burnetii* [10]. We optimized this application for the detection of cytopathic effects caused by coronavirus disease 2019 (COVID-19).

Briefly, a database consisting of negative (uninfected cells) and positive (infected cells) controls was generated. The data were used to define specific features allowing discrimination between the two groups. The following features were selected: the average, total and variation of the nuclear fluorescence intensity per cell, the nuclear area, the skewness of the bright-field intensity distribution, the kurtosis of the bright-field intensity distribution and the total intensity of the bright field within the regions of interest (ObjectAvgIntenCh1, ObjectTotalIntenCh1, ObjectVarIntenCh1, ObjectAreaCh1, ROI_SkewIntenCh3, ROI_KurtIntenCh3 and ROI_TotalIntenCh3, respectively). These parameters were used to generate two clusters using the K-means clustering algorithm, and the percentage of injured cells per well was calculated as previously described [10]. We then compared the percentage of injured cells obtained to the total cell count in each well to detect cell lysis using the formula ratio = (% injured cells/total cell count).

Large-scale co-culture of clinical samples

We applied this strategy for the detection of SARS-CoV-2 in 104 randomly chosen, anonymized nasopharyngeal swab samples. Initial RT-PCR ranged from 12 Ct to 34 Ct in 72 samples; 32 samples with negative initial PCR were used as negative controls. All samples except five were from hospitalized individuals. Sample preparation and co-culture were performed as previously described [11]. Briefly, 500 µL of the sample was processed into a 0.22-µm centrifugal filter (Merck Millipore, Darmstadt, Germany) and was centrifuged at 12 000 ***g*** for 5 minutes. Fifty microlitres was then inoculated on a monolayer of Vero E6 cells cultured in 96-well microplates. A negative control consisting of uninfected cells and a positive control consisting of cells infected with a 10^{-4} dilution of the IHUMI-3 strain were considered. A centrifugation step (700 ***g*** for 1 h) was performed to enhance the entrance of the virus into the cells. Plates were then incubated at 37°C and monitored for 7 days to search for cytopathic effects. In parallel, the same samples were processed using the classical isolation strategy based on the manual observation of cytopathic effects under an inverted microscope to validate our strategy [8,11,12]. For this strategy, co-cultures showing no cytopathic effects after 1 week were sub-cultured at days 7 and 14 onto a fresh monolayer of cells for a complete observation of 3 weeks.

Results validation by scanning electron microscopy and RT-PCR

Positive co-cultures were processed with both scanning electron microscopy (SEM) and RT-PCR directly from culture supernatant to validate the presence of COVID-19 viral particles. Briefly, SEM was performed using the SU5000 microscope (Hitachi High-Tech Corporation, Tokyo, Japan) allowing a rapid observation in approximately 10 minutes without time-consuming sample preparations [12]. The RT-PCR protocol was performed as previously described by Amrane et al., targeting the E gene [13]. This RT-PCR was applied to wells showing a cytopathic effect to confirm that this effect was due to SARS-CoV-2, and to negative wells to confirm that the lack of cytopathic effect was not due to microscopically undetectable minimal viral growth.

Statistical analysis

The R Studio® and XLSTAT software programs were used to perform all statistical tests included in this paper. Values of p were calculated to search for significant differences between the positivity rates obtained on a daily basis of co-culture using the HCS and the classic isolation strategies. Receiver operating characteristic curves were also calculated to determine a positivity threshold for strain isolation related to the initial viral load in the samples (initial RT-PCR results on the samples) for the two strategies. These

evaluations were performed on all 104 nasopharyngeal swab samples tested in this work.

Ethics statement

According to the procedures of the French Commission for Data Protection (Commission Nationale de l'Informatique et des Libertés), collected data were anonymized. The study was approved by the local ethics committee of IHU (Institut Hospitalo-Universitaire) - Méditerranée Infection (No. 2020-01).

Results

Cytopathic effects and cell lysis detection

Fig. 1 presents the fluorescence and bright-field images acquired with the CX7 microscope at days 1 and 6 post infection, showing the early stages of infection of SARS-CoV-2 (see Supplementary material, Fig. 1a,b) compared with advanced stages of infection and cell lysis (see Supplementary material, Fig. 1g—k). Typical cytopathic effects consist of an increasing nuclear fluorescence

intensity of the NucBlue fluorescent probe, in addition to nuclear fragmentation. These observations resulted in increases in the average, total and variation intensities of the nucleus and a decrease in the nuclear area on the fluorescence images. Additionally, infected cells become round and form aggregates, resulting in increases in total intensity, skewness and kurtosis on the bright-field images. Finally, advanced stages of infection are represented by cell lysis.

Automated detection results

The data extracted from the images were analysed in the dedicated application in R Studio. The database of negative and positive controls served as training data for the clustering algorithm, and a baseline of 2%—3% injured cells was predicted in the negative training data compared with a value of 50%—55% injured cells in the positive training data. The percentage of injured cells in each condition was predicted and then divided by the total cell count per well. This ratio allowed us to distinguish positive wells, showing cytopathic effects or cell lysis, from the negative control wells consisting of uninfected cells (Fig. 1a). Cytopathic effects were
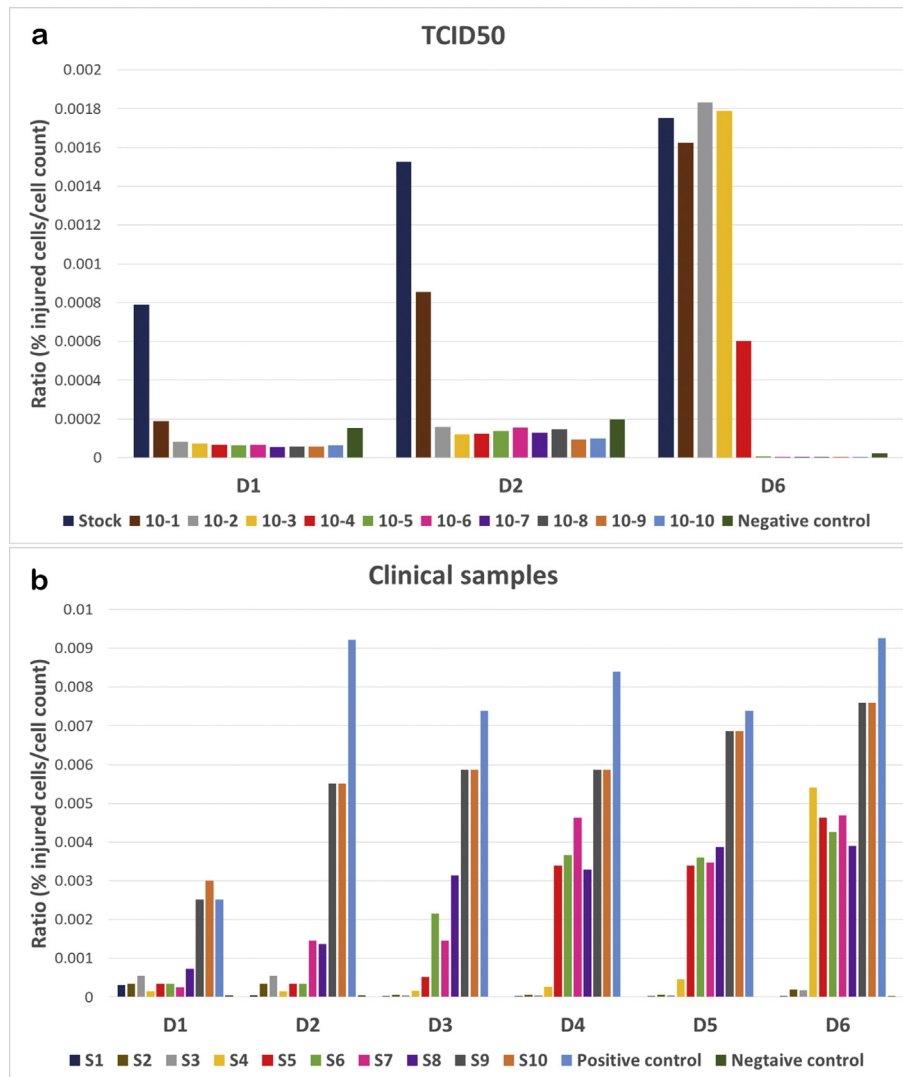

Fig. 1. Automated detection of severe acute respiratory syndrome coronavirus 2 (SARS-CoV-2) in co-culture. (a) Ratio of the percentage of injured cells on the total cell count of SARS-CoV-2-infected cells at different concentrations compared with the negative control over a period of 6 days. (b) Ratio of the percentage of injured cells on the total cell count of ten clinical samples with different initial viral loads over a period of 6 days. Initial viral loads were negative in S1 and S2, 32 Ct in S3, 30 Ct in S4, 29 Ct in S5, 28 Ct in S6, 23 Ct in S7, 22 Ct in S8, 16 Ct in S9 and 15 Ct in S10.
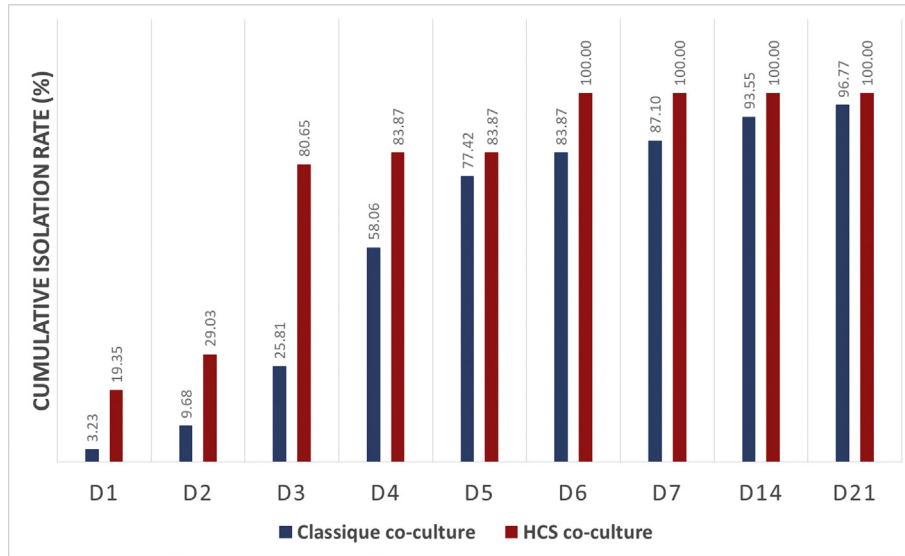
Fig. 2. Cumulative percentage of isolated strains per day using the classic and the new high-content screening isolation strategies for samples detected as positive in co-culture.
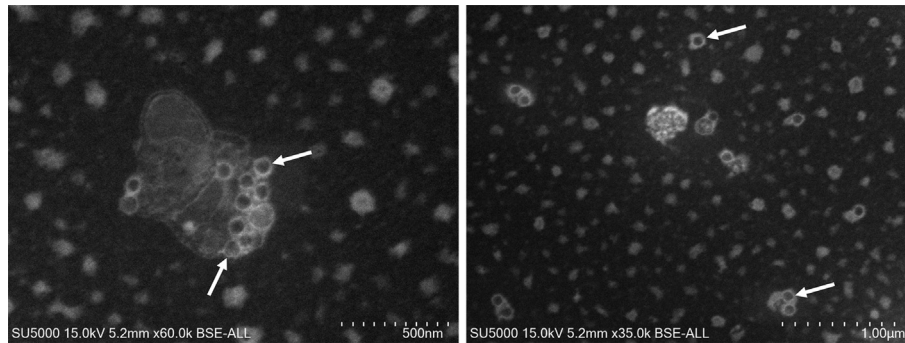

Fig. 3. Scanning electron microscopy images obtained with the SU5000 microscope showing severe acute respiratory syndrome coronavirus 2 (SARS-CoV-2) particles isolated from clinical samples (white arrows). Acquisition settings and scale bars are generated on the original micrographs.
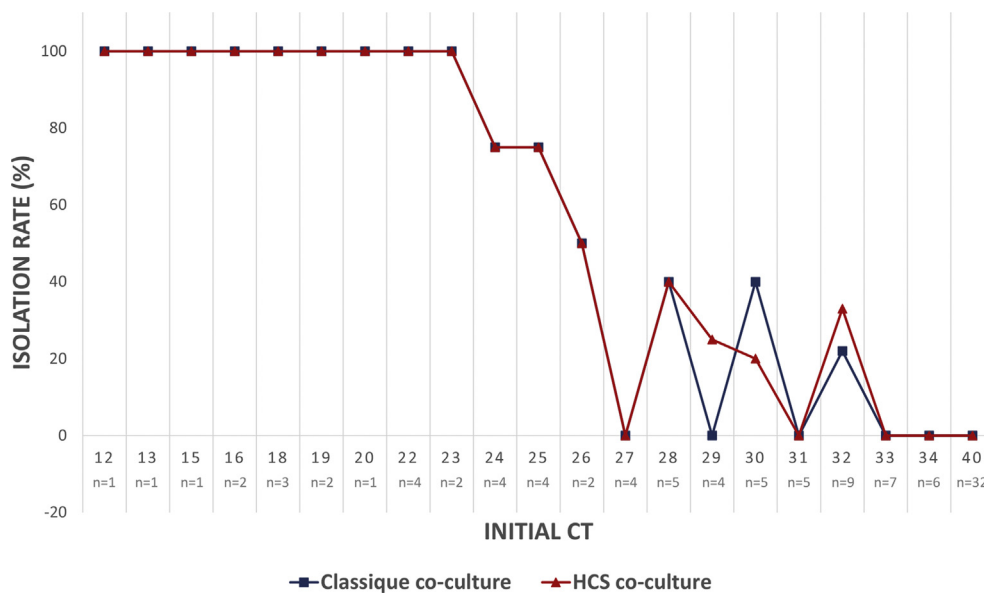

Fig. 4. Isolation rate of severe acute respiratory syndrome coronavirus 2 (SARS-CoV-2) from nasopharyngeal samples according to initial Ct values in samples using the classic and the new high-content screening isolation strategies (40 Ct represents the samples with a negative initial PCR). Note that the curves are overlapping before 28 Ct, showing similar isolation rates for both strategies.

detectable up until the dilution 10^{-4} after 6 days of culture for the strain IHUMI-3 used in this study, which corresponds to the viral titre obtained by $TCID_{50}$.

Furthermore, the automation system allowed us to monitor co-culture on a daily basis without any intervention from the operators. The Momentum software was used to monitor the automation system linked to the HCS microscope. A screening process was predefined, which allowed the proper incubation of the plates followed by the automated handling of the screening process at each specified time-point.

Screening of clinical samples with the new HCS and the classic isolation strategies

Among the panel of 104 samples processed on the CX7 microscope, 32 samples had a negative initial PCR and were considered controls for the system's sensitivity; therefore, the corresponding co-cultures were negative. Among the remaining 72 samples, we managed to isolate the virus from 31 samples using our automated detection system. The detection delay ranged from 24 hours to 3 days for most samples and was prolonged to 6 days for samples with low viral load. Fig. 1b shows examples of co-culture results obtained with the automated detection system compared with the negative (uninfected cells) and positive (cells infected with the viral strain IHUMI-3) controls.

Regarding the classic isolation strategy, 30 viral strains were isolated from the tested panel of samples, and the 32 samples with negative initial PCR had negative culture results as well. The majority of strains were recovered after 4 days of co-culture, and only a few were isolated at earlier stages. Three strains out of 30 were recovered after subcultures, two in the second week and one in the third week of co-culture.

A significantly higher percentage of positive samples was observed on a daily basis with the HCS strategy (Fig. 2). Moreover, the majority of positive samples were isolated by the third day of co-culture using the HCS strategy, where 80% (25/31) positivity was obtained compared with only 26% (8/30) with the classic strategy (p < 0.001).

To validate our results, positive co-cultures were processed for SEM to confirm the presence of viral particles. We detected viral particles in the supernatants of all samples that were detected as positive by the HCS strategy. Fig. 3 shows an example of particle
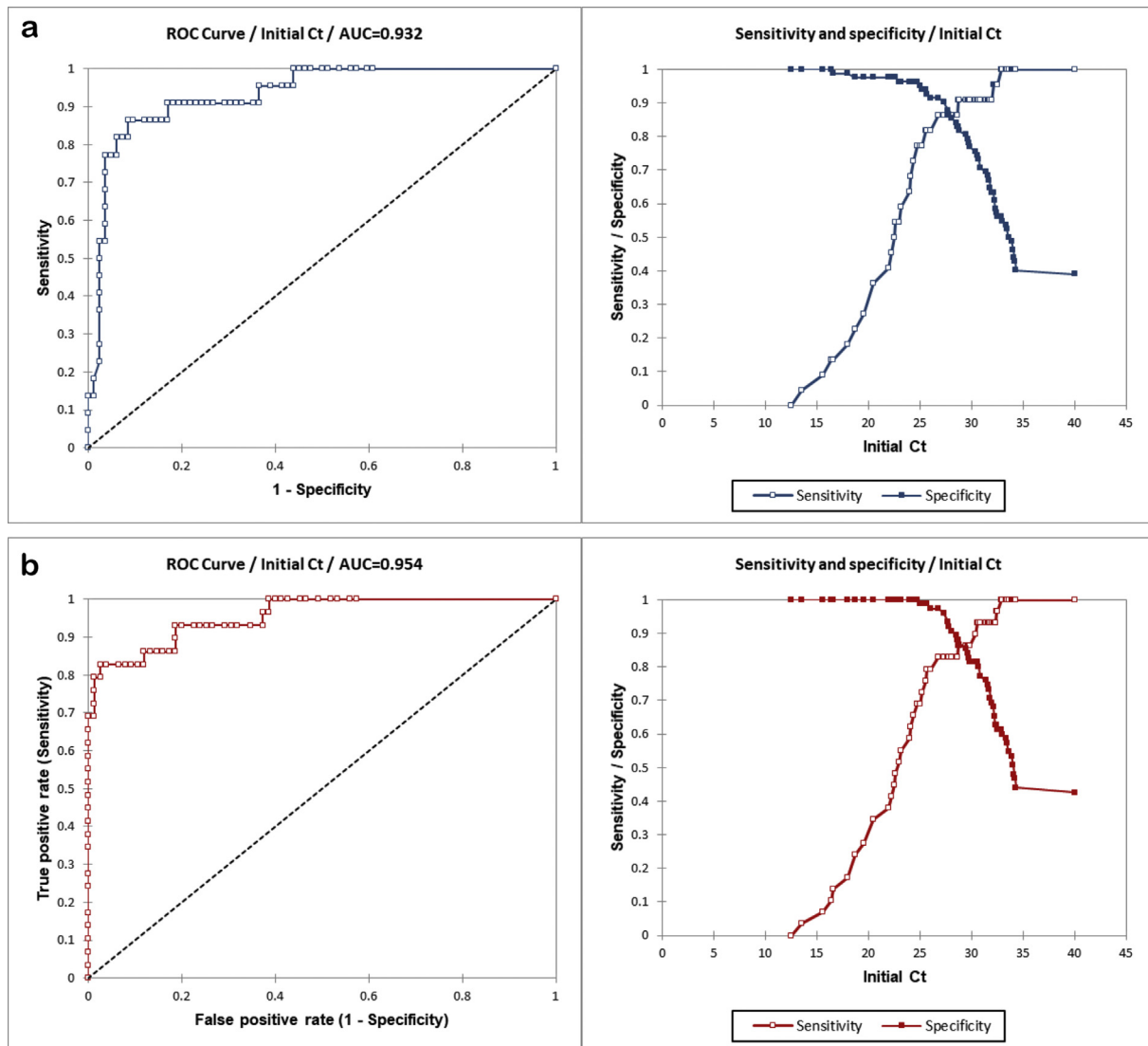

Fig. 5. Receiver operating characteristics curves and positivity threshold analysis for positive samples detected by the classic (a) and the high-content screening (b) isolation strategies.

detection in culture supernatant by SEM. RT-PCR performed on all wells correlated with the results of the microscopy-based detection.

Then, we correlated the isolation rates obtained with both strategies to the initial viral load (RT-PCR results) in each sample (Fig. 4). We obtained similar isolation rates with the HCS isolation strategy and the classic strategy. Moreover, we observed that most of the strains were recovered from samples with an initial viral load lower than 30 Ct with both strategies, and in most cases, isolation failed from samples with higher Ct values. Therefore, we calculated the positivity threshold of the isolation rate compared with the initial viral load in the samples using an ROC curve, and we obtained a similar positivity threshold of 27 Ct for both isolation strategies (Fig. 5).

Discussion

In this work, we were able to co-culture a large amount of clinical samples and monitor them with a fully automated system, which reduced the workload and time required from laboratory technicians. Similar isolation rates were obtained with both isolation strategies, which validated the efficiency of our new automated system. Moreover, this isolation rate was obtained in 1 week with the HCS strategy without any further subcultures, contrary to the classic technique with weekly subcultures for a total incubation time of 3 weeks. The main advantage of this technique relies on the automation, as it limits the risks of exposure or contamination of the personnel, as plate monitoring and data analysis can be carried out from a distance, so avoiding direct contact and manual observations of co-cultures. Furthermore, the loss of virus cultivability in samples allows us to consider the patients to be at low risk of contamination, which helps in the decision-making to discharge these individuals from the infectious diseases wards [8]. The use of the HCS isolation strategy allowed us to answer this question in 1 week. This is especially critical at the beginning of an epidemic or when PCR detection systems have to be modified. Moreover, several studies showed that assessing the duration of SARS-CoV-2 infectivity is based on viral cell culture or secondary infection rates [12,14—19]. Therefore, our automated isolation system allows us to answer this question faster than any other tool, and viral infectivity can be assessed several times during the outbreak to search for modifications, such as reduced transmissibility or effect of antiviral therapy. Furthermore, the greater the number of strains isolated, the better the understanding of the genetic diversity of this virus, especially as genome sequencing directly from samples is limited to the viral load, and a very poor genome assembly is obtained when the viral load is greater than 19 Ct [19,20]. Subsequently, developing an automated viral isolation technique was necessary to overcome the subjective and time-consuming manual microscopic observations. This new strategy is therefore applicable during the current crisis to recover strains from suspected samples in a safe and rapid way. Further work is underway to apply this technique for the large-scale drug susceptibility testing of SARS-CoV-2 strains isolated from patients. Finally, the algorithms used here could be adapted and applied for the detection and isolation of other viruses from clinical samples in cases of known and emerging viral diseases.

Transparency declaration

The authors would like to declare that Didier Raoult is a consultant for Hitachi High-Tech Corporation.

Author contributions

JYBK and BLS conceived the project. RF and JYBK developed the HCS methodology. RF, MLB, PJ and CG conducted the experiments. RF and JYBK conducted the analysis. RF, DR, JYBK and BLS wrote the manuscript.

Appendix A. Supplementary data

Supplementary data to this article can be found online at https://doi.org/10.1016/j.cmi.2020.09.018.

References

[1] WHO. Director-General's opening remarks at the Mission briefing on COVID-19. 2020. n.d. Available from: https://www.who.int/dg/speeches/detail/who-director-general-s-opening-remarks-at-the-mission-briefing-on-covid-19 12-march-2020. [Accessed 2 April 2020].

[2] Lai CC, Shih TP, Ko WC, Tang HJ, Hsueh PR. Severe acute respiratory syndrome coronavirus 2 (SARS-CoV-2) and coronavirus disease-2019 (COVID-19): the epidemic and the challenges. Int J Antimicrob Agents 2020;55:105924.

[3] Zhu N, Zhang D, Wang W, Li X, Yang B, Song J, et al. A novel coronavirus from patients with pneumonia in China, 2019. N Engl J Med 2020;382:727—33.

[4] Tang Y-W, Schmitz JE, Persing DH, Stratton CW. The laboratory diagnosis of COVID-19 infection: current issues and challenges. J Clin Microbiol 2020. https://doi.org/10.1128/JCM.00512-20. epub ahead of print.

[5] Chu DKW, Pan Y, Cheng SMS, Hui KPY, Krishnan P, Liu Y, et al. Molecular diagnosis of a novel coronavirus (2019-nCoV) causing an outbreak of pneumonia. Clin Chem 2020;66:549—55.

[6] Chan JF-W, Yip CC-Y, To KK-W, Tang TH-C, Wong SC-Y, Leung K-H, et al. Improved molecular diagnosis of COVID-19 by the novel, highly sensitive and specific COVID-19-RdRp/Hel real-time reverse transcription-polymerase chain reaction assay validated in vitro and with clinical specimens. J Clin Microbiol 2020. https://doi.org/10.1128/jcm.00310-20. epub ahead of print.

[7] Wang L-S, Wang Y-R, Ye D-W, Liu Q-Q. A review of the 2019 novel coronavirus (COVID-19) based on current evidence. Int J Antimicrob Agents 2020:105948. https://doi.org/10.1016/j.ijantimicag.2020.105948.

[8] La Scola B, Le Bideau M, Andreani J, Hoang VT, Grimaldier C, Colson P, et al. Viral RNA load as determined by cell culture as a management tool for discharge of SARS-CoV-2 patients from infectious disease wards. Eur J Clin Microbiol Infect Dis Off Publ Eur Soc Clin Microbiol 2020. https://doi.org/10.1007/s10096-020-03913-9. epub ahead of print.

[9] Francis R, Ominami Y, Bou Khalil JY, La Scola B. High-throughput isolation of giant viruses using high-content screening. Commun Biol 2019. https://doi.org/10.1038/s42003-019-0475-6. epub ahead of print.

[10] Francis R, Mioulane M, Le Bideau M, Mati M-C, Fournier P-E, Raoult D, et al. High-Content screening, a reliable system for Coxiella burnetii isolation from clinical samples. J Clin Microbiol 2020;58. https://doi.org/10.1128/jcm.02081-19.

[11] Gautret P, Lagier J-C, Parola P, Hoang VT, Meddeb L, Mailhe M, et al. Hydroxychloroquine and azithromycin as a treatment of COVID-19: results of an open-label non-randomized clinical trial. Int J Antimicrob Agents 2020: 105949. https://doi.org/10.1016/j.ijantimicag.2020.105949.

[12] Colson P, Lagier JC, Baudoin JP, Bou Khalil J, La Scola B, Raoult D. Ultrarapid diagnosis, microscope imaging, genome sequencing, and culture isolation of SARS-CoV-2. Eur J Clin Microbiol Infect Dis 2020;39:1601—3.

[13] Amrane S, Tissot-Dupont H, Doudier B, Eldin C, Hocquart M, Mailhe M, et al. Rapid viral diagnosis and ambulatory management of suspected COVID-19 cases presenting at the infectious diseases referral hospital in Marseille, France, January 31st to March 1st, 2020: a respiratory virus snapshot. Travel Med Infect Dis 2020:101632. https://doi.org/10.1016/j.tmaid.2020.101632.

[14] Wölfel R, Corman VM, Guggemos W, Seilmaier M, Zange S, Müller MA, et al. Virological assessment of hospitalized patients with COVID-2019. Nature 2020;581:465—9.

[15] Young BE, Ong SWX, Ng LF, Anderson DE, Chia WN, Chia PY, et al. Immunological and viral correlates of COVID-19 disease severity: a prospective cohort study of the first 100 patients in Singapore. SSRN Electron J 2020. https://doi.org/10.2139/ssrn.3576846. epub ahead of print.

[16] Million M, Lagier JC, Gautret P, Colson P, Fournier PE, Amrane S, et al. Early treatment of COVID-19 patients with hydroxychloroquine and azithromycin: a retrospective analysis of 1061 cases in Marseille, France. Travel Med Infect Dis 2020;35. https://doi.org/10.1016/j.tmaid.2020.101738.

[17] Bullard J, Dust K, Funk D, Strong JE, Alexander D, Garnett L, et al. Predicting infectious SARS-CoV-2 from diagnostic samples. Clin Infect Dis 2020. https://doi.org/10.1093/cid/ciaa638.

[18] Kampen JJA van, Vijver DAMC van de, Fraaij PLA, Haagmans BL, Lamers MM, Okba N, et al. Shedding of infectious virus in hospitalized patients with coronavirus disease-2019 (COVID-19): duration and key determinants. MedRxiv 2020;2019:2020.

[19] Lu J, Peng J, Xiong Q, Liu Z, Lin H, Tan X, et al. Clinical immunological and virological characterization of COVID-19 patients that test re-positive for SARS-CoV-2 by RT-PCR. Medrxiv 2020:1—26. https://doi.org/10.1101/2020.06.15.20131748.

[20] Ahn D-G, Shin H-J, Kim M-H, Lee S, Kim H-S, Myoung J, et al. Current status of epidemiology, diagnosis, therapeutics, and vaccines for novel coronavirus disease 2019 (COVID-19). J Microbiol Biotechnol 2020;30:313—24.